

A Comparison of Extended Kalman Filter, Extended Information Filter, and Least Squares Approaches for Parameter Identification of a Transient Heat Transfer Problem

M.R. Myers*, A.B. Jorge[†], D.G. Walker*, M.J. Mutton[‡]

*Department of Mechanical Engineering, Vanderbilt University, Nashville, TN, 37235, Email: Mike.Myers@Vanderbilt.Edu

[†]Mechanical Engineering Institute, Federal University of Itajubá, Itajubá, MG, Brazil

[‡]Industrial Measurement Systems, Inc., 2760 Beverly Drive, Suite 4, Aurora, IL 60502

INTRODUCTION

Knowledge of where air flowing across a body transitions from laminar flow to turbulent flow can provide numerous benefits to air vehicle design, thermal protection system design, and air vehicle in-flight control [1]. At the transition between these two flow regimes, a change in body-surface temperature has been measured [2]. The objective of this work is to develop a method to locate and characterize the heat flux change induced by the boundary layer transition. The solution involves a forward conduction solution and an inverse procedure. The work presented here focuses on forward conduction solution, flat plate experimentation with a known heat source, and parameter identification of the applied heat flux and the convection coefficient. Three inversion approaches are compared: extended Kalman filter, extended information filter, and least squares.

FORWARD CONDUCTION SOLUTION AND VERIFICATION

This work focuses first on a large flat plate heated over a small area with a known heat source. Consider a 61cm x 30.5cm x .635cm stainless steel 316L plate with constant properties of $k = 15$ W/m K, $C_p = 500$ J/kg K and $\rho = 8,000$ kg/m³ (Figure 1). The heating source is fixed at the plate center, is applied at $t = 300$ sec and removed at $t = 600$ sec, and has a heating profile of $q = 1.7$ MW/m² over 0.635 cm diameter circular area. Radiation effects are assumed to be negligible.

The model uses a finite element mesh with smaller elements near the heat source and larger elements near the plate edges to conserve computing resources. A grid convergence study was performed to ensure grid independence. This study led to the selection of three mesh layers through the plate's thickness dimension, 9,780 total elements, and 45,983 degrees of freedom. Independent verification of the numerical solution obtained from COMSOL Multiphysics by the COMSOL Group was performed using a closed-form, analytical solution of heating through a circular domain without convection [3]. Agreement between the COMSOL solution and the closed-form solution is acceptable with mean absolute error less than 0.5 K.

FLAT PLATE EXPERIMENT

Eight K-type thermocouples were attached to a 61cm x 30.5cm x 0.635cm plate of stainless steel 316L. The plate was sized such that the plate edges would not affect the temperature profile in the plate during the experiment. Four thermocouples were attached on one side and four on the other. With plate center being the origin and the x -axis being the length (Figure 1), thermocouples were attached at (x, y) locations of (1cm, 1cm), (2cm, 2cm), (3cm, 3cm), and (-1cm, -1cm) on the heated side ($z = 0$) and on the non-heated side ($z=0.00635$ m). The desire was to have thermocouple pairs in exactly the same position on either side of the plate allowing measurement of the temperature difference between the two sides. The thermocouples were secured to the plate with thermal grease and Kapton tape to ensure good thermal contact. Flat black paint was applied to a circular area at the plate center to maximize energy absorption from the heater. The plate was oriented vertically with the positive y -axis pointing up. A Research, Inc. SpotIR 4150 heater with focusing cone was positioned approximately 2mm from the plate surface such that its beam struck the plate center. Experiments were conducted with the heater running at full-power which, according to manufacturer's specifications, produces 1.7 MW/m² of heat flux on the plate in a circular area 0.635 cm in diameter. Consequently, approximately 54 Watts of energy are being absorbed by the plate when the heater is on.

During the experiment, the heater is turned on at $t = 300$ seconds and turned off and removed at $t = 600$ seconds. Data acquisition equipment was used to record thermocouple temperature readings every second during the experiment. A MIKRON Thermo Scan TS7302 infrared camera was used to collect thermal images of the plate and heater. Coupled with a laptop computer, this system recorded thermal images every five seconds during the experiment.

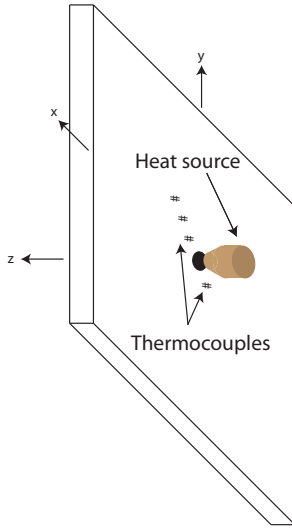


Fig. 1. Illustration of flat plate with heat source and sensors (not drawn to scale).

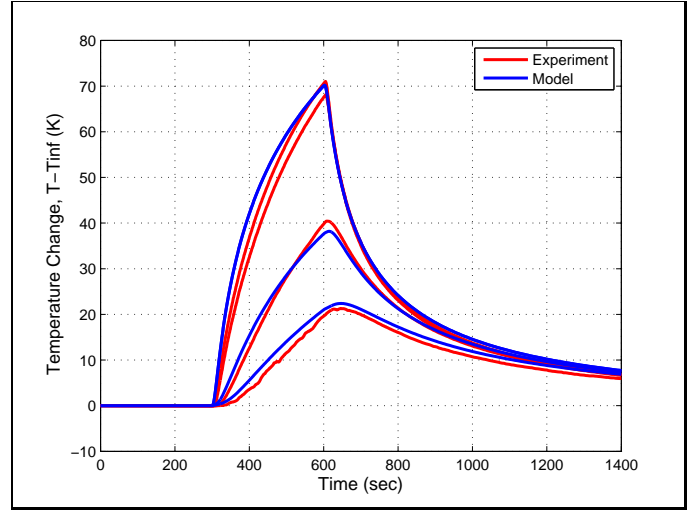


Fig. 2. Temperature response on non-heated side of the plate at four sensor locations.

PARAMETER IDENTIFICATION

Even with manufacturer specifications, the heat transfer between the radiative heater and the plate is not known with much certainty. Further complicating matters, the heater's proximity to the plate implies an unknown amount of secondary radiation and convection heating on the plate. The focusing cone reaches temperatures in excess of 200°C and the lamp is cooled with forced air that exits the heater through the focusing cone pointed at the plate. For this initial analysis, the main heat flux and convection coefficient are estimated. The secondary heating is modeled with a Gaussian profile of $q''_g = 100 \text{ W/m}^2$ and $\sigma_g^2 = 0.0009 \text{ m}$. h is assumed constant and identical on both sides of the plate. Estimating h using free convection correlations [4] produces an expected range of $2 \text{ W/m}^2\text{K} \leq h \leq 5 \text{ W/m}^2\text{K}$. Since the plate edges do not contribute significantly to the boundary, $h = 3 \text{ W/m}^2\text{K}$ is assumed on all four plate edges.

Three inverse methods are compared to quantify the heat flux (q) and convection coefficient (h) on the plate: least squares, extended Kalman filter, and extended information filter. The extended Kalman filter and extended information filter are members of a family of recursive state estimators, collectively called Gaussian filters [5]. The extended information filter is the information form of the Kalman filter. Both filters linearize nonlinear Gaussian systems. For the inversion, the entire experiment is treated as one event, and all temperature measurements are combined together. The 5,056 temperature measurements therefore are effectively 5,056 separate sensors. All three methods start with an initial guess of the state $x_0 = [q \ h]^T = [1.7 \text{ MW/m}^2 \ 5.0 \text{ W/m}^2\text{K}]^T$ and are processed recursively to convergence.

The least squares estimator is $x_{new} = x + (X_{\beta}^T X_{\beta})^{-1} X_{\beta}^T (Y - T|_x)$ where X is the Jacobian based on finite differences obtained by independently varying the state parameters 0.1%, Y are the experimentally obtained temperatures, and $T|_x$ are temperatures based on current estimates for the state x [6]. The Jacobian was normalized to produce a better conditioned matrix. For the extended Kalman filter, there is no input to the state thus the state model is $a = I_2$ and the state Jacobian is $A = I_2$, where I_2 is a 2×2 identity matrix. The measurement model b consists of the temperature measurements, which is a $5,056 \times 1$ matrix, and the measurement Jacobian B is obtained using finite differences (a $5,056 \times 2$ matrix) by independently varying the state parameters 0.1%. The state covariance matrix R is a 2×2 diagonal matrix using $\sigma_q^2 = 0.1 \text{ MW}^2/\text{m}^4$ and $\sigma_h^2 = 0.1 \text{ W}^2/\text{m}^4\text{K}^2$. These values were chosen to achieve smooth convergence behavior since small values for the state covariance matrix cause the Gaussian filters to diverge while arbitrarily large values for the state covariance matrix render the Gaussian filters essentially identical to the least squares method. The thermocouples have a measurement accuracy of $\pm 1.5^{\circ}\text{C}$, which translates to a measurement variance of $\sigma_T^2 = 0.25^{\circ}\text{C}^2$. This value was used for the diagonal elements of the measurement covariance matrix Q , a $5,056 \times 5,056$ matrix. The filter is initialized with the initial state x_0 (stated above) and covariance $\Sigma_0 = 0$. For the extended information filter, a , A , b , B , R , and Q are identical to those in the extended Kalman filter. The extended information filter possesses an advantage of allowing Q^{-1} to be computed once and reused for all iterations. Because the initial state covariance matrix Σ_0 is inverted in the extended information filter, the filter was initialized with $\Sigma_0 = R$ instead of the zero matrix used to initialize the extended Kalman filter.

Figures 3 and 4 illustrate the convergence behavior for all three methods. The extended Kalman filter and extended information filter converge identically and are presented together. The Gaussian filters converge a bit slower than the least squares method, however the convergence is smoother. Once convergence was achieved, statistical moments were computed from the last three

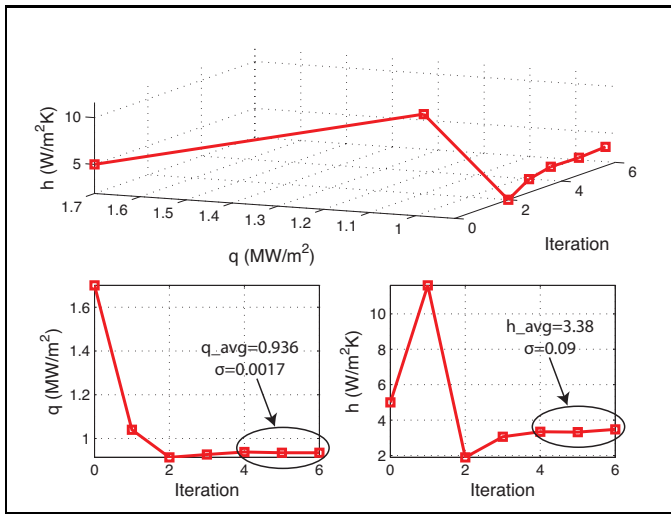


Fig. 3. Least squares convergence.

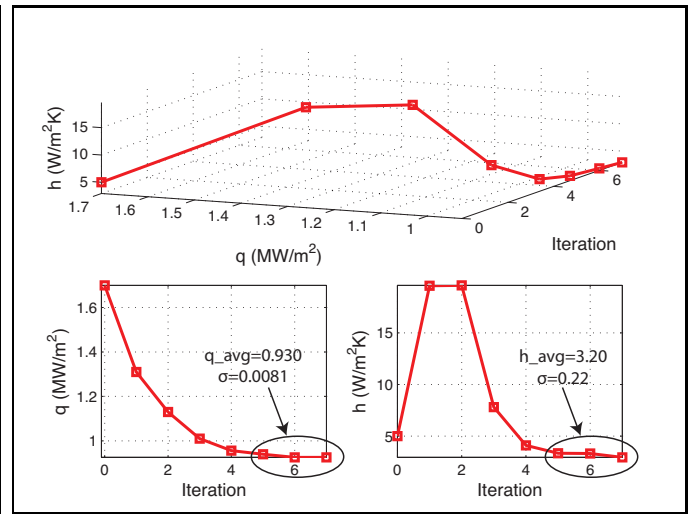


Fig. 4. Extended Kalman filter and extended information filter convergence. The filters produce identical results and are presented together.

iterations. Results are similar for all three methods. Computational cost is lowest with least squares, followed by extended information filter, and then extended Kalman filter. Figure 2 compares the temperature response measured during the experiment with the temperature response of the model using $q = 0.930 \text{ MW/m}^2$ and $h = 3.20 \text{ W/m}^2 \text{ K}$. Discrepancies between the two thermocouple sets closest to the source [(1cm, 1cm) and (-1cm, -1cm)] arise from sensor placement error. Agreement between the model and the experiment is acceptable, however improvement could be achieved through modifications to the heating profile (e.g., secondary heating). A check of the boundary effect errors was conducted to ensure the plate was sized sufficiently large. Of particular interest is in the region of $(\pm 4\text{cm}, \pm 4\text{cm})$ where the errors remain well below 0.5% for the entire experiment. Even at $(\pm 10\text{cm}, \pm 10\text{cm})$, the errors are below 1% for much of the experiment and stay below 3% for the entire experiment. Solution sensitivity analysis was performed to find $\partial T/\partial q$ and $\partial T/\partial h$ versus time using finite differences. This analysis indicates q and h are not correlated and q dominates the solution.

CONCLUSIONS

Results were presented from forward conduction solution development, flat plate experimentation with a known heat source, and parameter identification of heat flux and convection coefficient on the plate. Least squares, extended Kalman filter, and extended information filter inversion methods produced similar results. This finding is significant as future work will add more free parameters (e.g., secondary heating profile) and heat source localization to the inverse procedure. Whereas this work had no inputs to the state model, the ability to add inputs to a recursive state estimator (e.g., a Gaussian filter) is anticipated to be more robust for heat source localization and in turn for boundary layer transition localization and characterization.

REFERENCES

- [1] H. L. Reed, R. L. Kimmel, S. Schneider, D. Arnal, and W. Saric, "Drag prediction and transition in hypersonic flow," in *Symposium on Sustained Hypersonic Flight, AGARD Conference on Future Aerospace Technology in the Service of the Alliance*, 1997.
- [2] T. J. Horvath, S. A. Berry, and B. R. Hollis, "Boundary layer transition on slender cones in conventional and low disturbance mach 6 wind tunnels," in *32nd AIAA Fluid Dynamics Conference and Exhibit*, 2002.
- [3] V. Kozlov, V. Adamchik, and V. Lipovtsev, "Local heating of an unbounded orthotropic plate through a circular and annular domain," *Journal of Engineering Physics and Thermophysics*, Jan 1989.
- [4] F. P. Incropera and D. P. DeWitt, *Introduction to Heat Transfer*, 4th ed. John Wiley and Sons, 2002.
- [5] S. Thrun, W. Burgard, and D. Fox, *Probabilistic Robotics*. The MIT Press, 2006.
- [6] K. A. Woodbury, "Sequential function specification method using future times for function estimation," in *Inverse Engineering Handbook*, K. A. Woodbury, Ed. CRC Press, 2003.